

Speckles generated by skewed, short-coherence light beams

This article has been downloaded from IOPscience. Please scroll down to see the full text article.

2011 New J. Phys. 13 123007

(<http://iopscience.iop.org/1367-2630/13/12/123007>)

View [the table of contents for this issue](#), or go to the [journal homepage](#) for more

Download details:

IP Address: 134.21.47.136

The article was downloaded on 02/03/2012 at 07:52

Please note that [terms and conditions apply](#).

Speckles generated by skewed, short-coherence light beams

D Brogioli^{1,3}, D Salerno¹, F Croccolo², R Ziano¹
and F Mantegazza¹

¹ Dipartimento di Medicina Sperimentale, Università degli Studi di Milano—Bicocca, Via Cadore 48, Monza (MB) 20900, Italy

² Physics Department, University of Fribourg, Ch du Musée 3, 1700 Fribourg, Switzerland

E-mail: dbrogioli@gmail.com

New Journal of Physics **13** (2011) 123007 (9pp)

Received 6 September 2011

Published 6 December 2011

Online at <http://www.njp.org/>

doi:10.1088/1367-2630/13/12/123007

Abstract. When a coherent laser beam impinges on a random sample (e.g. a colloidal suspension), the scattered light exhibits characteristic speckles. If the temporal coherence of the light source is too short, then the speckles disappear, along with the possibility of performing homodyne or heterodyne scattering detection or photon correlation spectroscopy. Here we investigate the scattering of a so-called ‘skewed coherence beam’, i.e. a short-coherence beam modified such that the field is coherent within slabs that are skewed with respect to the wave fronts. We show that such a beam generates speckles and can be used for heterodyne scattering detection, despite its short temporal coherence. Moreover, we show that the heterodyne signal is not affected by multiple scattering. We suggest that the phenomenon presented here can be used as a means of carrying out heterodyne scattering measurement with any short-coherence radiation, including x-rays.

³ Author to whom any correspondence should be addressed.

Contents

1. Introduction	2
2. The experimental setup	2
3. Experimental results	3
4. Discussion	4
5. Applications	7
6. Conclusions	8
Acknowledgments	8
References	8

1. Introduction

Observing the light diffused from a scattering sample is a widely used, well-known tool applied to the study of biophysical systems, colloidal suspensions and complex fluids [1]. Homodyne dynamic light scattering and heterodyne detection are based on interference and, in particular, on the observation of speckle patterns. In this case, a long coherence is needed because the light path difference of the interfering beams must not exceed the coherence length. On the other hand, the disappearance of interference beyond the coherence length may be exploited to select a well-defined slab from a thick sample, for example in optical coherence tomography [2].

A single-mode laser beam has a very long longitudinal coherence and is transversely coherent across its section. In a beam with a short longitudinal coherence, the regions in which the electric field is correlated are slabs perpendicular to the beam direction. Using a dispersing optical element, it is possible to manipulate such a beam so that the coherent slabs are skewed by an angle σ with respect to the plane perpendicular to the beam direction [3]. This effect has been studied extensively in the context of ultra-short optical pulses [4, 5], and can be utilized to achieve more efficient nonlinear pulse generation (by increasing the phase-matching condition) [6, 7] or to avoid some linear side effects (such as group velocity mismatch and walk-off) [8].

In this paper, we describe the scattering of a skewed coherence beam by a random medium. In the near-field images of the sample, we observe that a skewed coherence beam gives rise to a speckle pattern that is not visible using short-coherence illumination, although the coherence length is identical. Thanks to the visibility of the speckle pattern, our experimental setup with the skewed coherence beam can be used as a so-called scattering in near-field (SINF) device [9, 10] that operates in a heterodyne detection configuration. Accordingly, we are able to obtain heterodyne light scattering measurements despite the short coherence of the illumination.

2. The experimental setup

Our short-coherence light source is a laser diode driven under threshold (Sacher Lasertechnik SAL-0660-025). The emission has a maximum at the wavelength of 660 nm, with an 8 nm full-width at half-maximum (FWHM) bandwidth. The regions of the emitted beam in which the field is coherent consist of thin slabs that are orthogonal to the direction of propagation and whose thickness equals the longitudinal coherence length (i.e. about 17 μm).

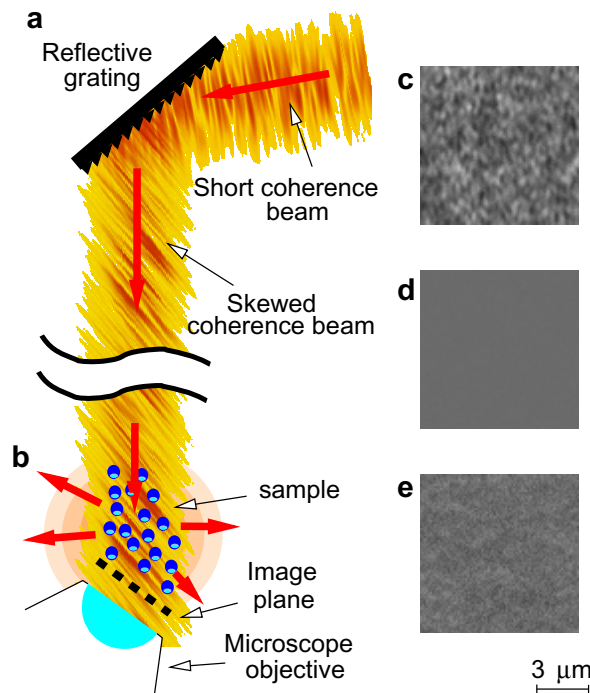


Figure 1. A schematic representation of the experimental setup. (a) Generation of the skewed beam. The coherent slabs of the original beam are perpendicular to the propagation direction. In the first-order diffracted beam the slabs are skewed with respect to the propagation direction. (b) The sample (colloidal suspension) and collection optics. Typical near-field images obtained with various beams are shown: a laser beam (c), a short coherence beam (d) and a skewed coherence beam with a skew angle of $\sigma = 47^\circ$ (e). The scattering medium is a water suspension of 80 nm polystyrene nanospheres.

To obtain the desired skewed coherence the beam is diffracted by a reflective grating [3, 5], with 600 lines per millimeter, blazed at 17.5° , and the first-order diffracted beam is selected (see figure 1(a)). In the resultant beam, the regions in which the field is coherent are slabs that are skewed (inclined) by an angle σ with respect to a direction perpendicular to the propagation direction [3, 5]. In our case, the skew angle σ can be adjusted from about $\sigma = 20^\circ$ to $\sigma = 50^\circ$ by changing the incidence angle of the beam with respect to the grating.

As shown in figure 1(b), the skewed beam passes through a 1-mm-thick cell containing the scattering sample (e.g. a colloidal suspension).

The intensity of the light in a plane close to the exit face of the cell is imaged by a charge-coupled device (CCD) camera (Luca Andor) through a high-numerical-aperture microscope objective (MO; Nikon CFI Plan Apochromat 63X NA 1.4), which collects both the transmitted and scattered beams (heterodyne detection).

3. Experimental results

The images obtained by illuminating the sample with a laser beam (figure 1(c)) clearly show the usual near-field speckle patterns [11, 12], with a strong contrast, due to the random interference

of the scattered beams. When a non-skewed beam (i.e. $\sigma = 0$) with a short temporal coherence is used (figure 1(d)), the speckles are almost invisible and appear extremely smeared because no interference can occur. Quite surprisingly, the images obtained with the skewed beams (i.e. $\sigma > 0$) do show speckles (figure 1(e)), although their texture is different from that observed for laser light.

To characterize the speckle fields, we evaluated the power spectra of the images obtained with beams skewed at various angles; the results are reported in figure 2. The power spectrum at $\sigma = 0$ exhibits a weak signal for the wave vectors \mathbf{q} close to the center of the Fourier-space image: this corresponds to the faint speckles. As the skew angle σ is increased, higher frequency modes appear in the images; in the power spectra, they appear as ellipses. The size of the ellipse in the power spectrum increases when the skew angle σ is increased.

These images can be interpreted as holograms of the scattered field. Each point in the near-field image (with wave vector \mathbf{q}) is generated by the interference between the most intense transmitted beam (with wave vector \mathbf{K}_I) and a single scattered beam (with wavevector \mathbf{K}_S). The relationship among \mathbf{K}_I , \mathbf{K}_S and \mathbf{q} is shown graphically in figure 2(e); the wave vector \mathbf{q} is the projection of the transferred wave vector $\mathbf{Q} = \mathbf{K}_S - \mathbf{K}_I$ in the image plane [13]. The SINF technique [9, 13–15] exploits this relationship to measure the scattering intensity by acquiring near-field images. In this case, the following observations can be made: (i) the observed ellipses correspond to scattering along a cone; (ii) the impinging beam direction is a generatrix of the cone; and (iii) the axis of the cone is orthogonal to the coherent slabs. In reality, the sample scatters at all angles, but only the scattering along the cone beats coherently with the local oscillator to provide a detectable heterodyne signal. Thus it will be called the ‘scattering detection cone’ (SDC).

Following the idea of SINF, we can recover the scattering intensities from the power spectra. The results for both a laser beam and a skewed coherence beam are shown in figure 3. In both cases, at a low volume fraction, the measured scattering intensity closely follows the Mie theory [16]. This shows that the detected light, scattered along the SDC, has the same direction and intensity as the light scattered by the particles, and the SDC acts only as a mask. By skewing the coherence, we can perform heterodyne detection, despite the short coherence of our light source.

When using laser light, we observe a progressive departure from the Mie theory for large scattering wave vectors [16], which can be easily interpreted as due to multiple scattering. In contrast, the use of the skewed beam (figure 3(b)) results in an almost perfect overlap between the data and the theoretical results on single scattering, independent of the nanoparticle concentration. This experiment shows that the use of skewed coherence beams in a heterodyne scattering detection setup suppresses the detection of multiple scattered light.

4. Discussion

Figure 4 presents a schematic explanation of the obtained results. A coherent slab impinges on a set of particles, which emit secondary waves. Interference only occurs when there is overlap between the coherent slab and the parts of the secondary waves that are coherent with it. In the section shown, overlap only occurs at two points, which define the two directions (indicated by arrows) along which the scattered waves interfere with the impinging beam. One is always along the forward direction, and the other is at a scattering angle of 2σ . This direction is identical for every particle. In three dimensions, the intersection of the coherent slab with the secondary

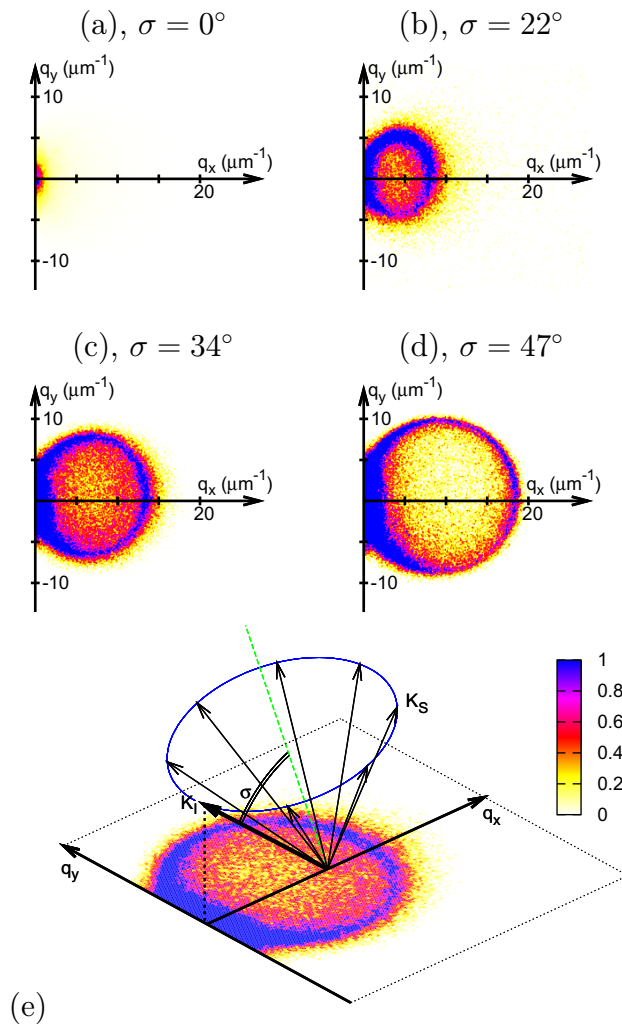


Figure 2. Power spectra. (a–d) Two-dimensional false-color power spectra of the near-field speckle patterns of the images obtained with an impinging beam with a short coherence, at various skew angles σ . (a) The spectrum of the image in figure 1(d), using a non-skewed beam. (b, c) Spectra of the images at skew angles $\sigma = 22^\circ$ and 34° . (d) The spectrum of the image in figure 1(e), using a skew angle of $\sigma = 47^\circ$. The scattering medium is a water suspension of 80 nm polystyrene particles. (e) A three-dimensional schematic diagram of the relationship among the wave vector \mathbf{K}_I of the impinging beam, the wave vectors \mathbf{K}_S of the scattered beams and the wave vectors $\mathbf{q} = (q_x, q_y)$ of the interference fringes in the image plane. The most intense points of the power spectrum are generated by light scattered along a cone, whose axis (green dashed line) is perpendicular to the coherent slabs.

spherical wave occurs along a circle, which defines a scattering cone with properties identical to those of the SDC.

From this simplified picture of the interference generated by a skewed beam, one can also infer why multiple scattering is not detected in this configuration. In fact, light that has been

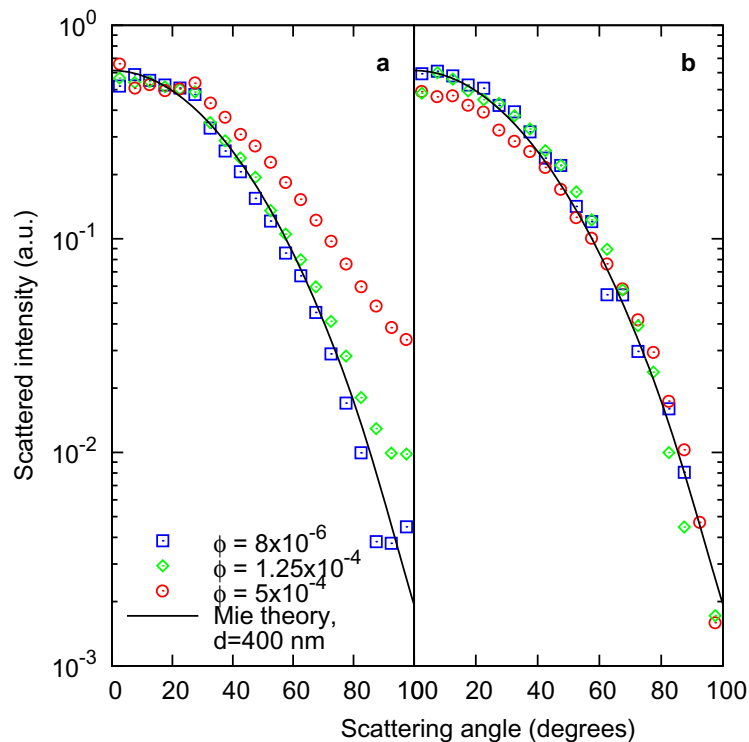


Figure 3. Measured scattering intensity. The sample consists of 400 nm polystyrene particles in water at various volume fractions ϕ . The data were obtained using a laser beam (a) or a skewed $\sigma = 47^\circ$ beam (b). The continuous line represents the Mie theory prediction for 400 nm dielectric spheres.

scattered more than once will arrive at the screen plane with a time shift greater than the beam's temporal coherence, thereby preventing interference.

When we take into account the thickness of the coherent slabs, we note that the secondary waves indeed interfere with the impinging beam for an interval of directions around $\vartheta = 2\sigma$, whose extent $\delta\vartheta$ increases as the distance from the coherent slab of the impinging beam to the emitting particle decreases. In particular, if we analyze a plane inside the sample, the particles whose distance from the detection plane is less than the coherence length can give a heterodyne signal at every angle. In other words, only a thin volume around the detection plane contributes to the scattering signal at a generic angle, but the whole volume of the sample contributes to the heterodyne signal along the SDC. This explains why the heterodyne signal along the SDC is much higher than that along other directions.

In general, the manipulation of the coherent slab allows us to select the volume of the sample that is detected: in our experiments, we are interested in extending this volume up to the whole sample; on the other hand, the so-called 'optical coherence tomography' [2] exploits the short coherence for selecting a well-defined slice of the sample (this is the meaning of 'tomography', namely 'drawing the image of a slice'). This view makes evident the deep analogy between the rejection of the multiple scattering in our experiment and the rejection of the slices other than the one selected in optical coherence tomography.

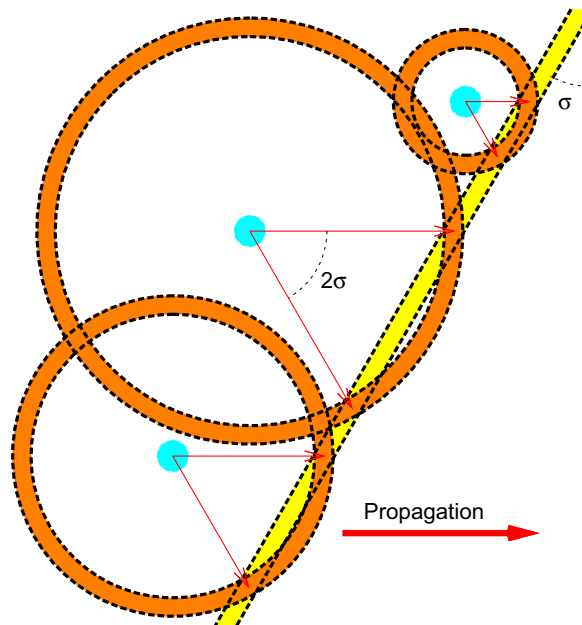


Figure 4. A qualitative interpretation of the scattering mechanism in the presence of a skewed beam. The impinging beam propagates from left to right in the direction shown by the arrow. The skewed coherent slab is shown as a yellow stripe. When it hits the particles (blue dots), secondary spherical waves are generated. The parts of the secondary wave that are coherent with the slab are the spherical shells (orange rings). Heterodyne interference is only observed where the coherent slab and the coherent spherical shells overlap.

5. Applications

Currently, the measurement of the skew angle of a sample beam is carried out using nonlinear optics and only in the case of ultra-short pulses with high energy⁴. However, the phenomenon described here enables the development of a much simpler technique based on observing the SDC in the power spectra; the axis of the SDC directly provides the normal to the coherence slabs. Such a technique would also be effective for faint beams and for both continuous waves and ultra-short pulses.

Furthermore, multiple scattering is a serious issue affecting scattering measurements, and several techniques have been developed to suppress the contributions of multiple scattering (see e.g. [17, 18] and references therein). This experiment shows that the use of skewed coherence beams in a heterodyne scattering detection setup suppresses multiple scattering and represents the most natural and effective way of reaching this target.

In the case of x-rays [19–23], the coherence conditions necessary for obtaining interference can be achieved by synchrotron radiation or FEL. However, this only occurs after filtering through a monochromator, which strongly reduces the photon flux. Our findings suggest that skewing the coherence of a short-coherence x-ray beam can enable heterodyne detection.

⁴ Single-shot autocorrelator ‘TIPA’ produced by Light Conversion (Vilnius, Lithuania), <http://www.lightcon.com/products/product.php?ID=115>

The actual optical scheme will depend on the application. For example, the main beam of a small-angle x-ray scattering (SAXS) apparatus can be used. In this case, the angular dispersion of the beam is much less than 1/1000 of radiant, which ensures a transversal coherence length of the order of microns, while the longitudinal coherence is of the order of a few nanometers. In order to obtain the skewed-coherence beam, a transversely coherent region of the main beam is selected by means of a pinhole; the resulting beam is sent through a transmission grating with a line spacing of the order of 100 nm, and the first-order diffracted beam is selected by a second pinhole. The resulting beam has a skew angle of the order of milliradians, and the corresponding SDC has an aperture of the same order, which is in the range usually detected with SAXS. The SINF detection scheme can still be applied with a variant of the method described above. Instead of taking an image of a plane, we will place an intensity mask (a transmission grating) on the same plane, with the wave vector we want to measure. The transmitted intensity will represent the amplitude of the corresponding Fourier mode of the image, and will represent the heterodyne signal.

6. Conclusions

We have shown that the use of a skewed-coherence beam allows us to detect a heterodyne signal with short-coherence light. We show that it is possible to skew the coherence of a short-coherence beam by means of an optical system including a diffraction grating. Anyhow, the skewing optical system does not increase the coherence length, nor does it act as a narrow-bandwidth filter. The detection is possible only for light scattered along the SDC, whereas the other scattering directions give a negligible heterodyne signal. The axis of the SDC is perpendicular to the coherent slabs and thus the detection of the SDC represents a very effective method of measuring the coherence skewness of either a continuous wave or a pulsed beam. When applied to quite turbid samples, the technique has the remarkable advantage of suppressing the multiple scattering contribution of the scattering signal. We suggest that the phenomenon presented here can be used as a means of carrying out heterodyne scattering measurement with any short-coherence radiation; the application of the technique to x-rays has also been discussed.

Acknowledgments

This work was partially financially supported by the European Union (EU): project NAD CP-IP 212043-2). FC acknowledges support from the EU (Marie Curie grant; contract IEF-251131; DyNeFl project).

References

- [1] Scheffold F and Cerbino R 2007 New trends in light scattering *Curr. Opin. Colloid Interface Sci.* **12** 50–7
- [2] Huang D *et al* 1991 Optical coherence tomography *Science* **254** 1178–81
- [3] Picozzi A and Haelterman M 2002 Hidden coherence along space-time trajectories in parametric wave mixing *Phys. Rev. Lett.* **88** 083901-1–4
- [4] Martinez O E 1986 Pulse distortions in tilted pulse schemes for ultrashort pulses *Opt. Commun.* **59** 229–32
- [5] Porras M A, Valiulis G and Di Trapani P 2003 Unified description of Bessel X waves with cone dispersion and tilted pulses *Phys. Rev. E* **68** 016613-1–11

- [6] Martinez O E 1989 Achromatic phase matching for second harmonic generation of femtosecond pulses *IEEE J. Quantum Electron.* **25** 2464–8
- [7] Szabo G and Bor Z 1990 Broadband frequency doubler for femtosecond pulses *Appl. Phys. B* **50** 51–4
- [8] Di P Trapani *et al* 1998 Observation of temporal solitons in second-harmonic generation with tilted pulses *Phys. Rev. Lett.* **81** 570–3
- [9] Brogioli D *et al* 2008 Nano-particle characterization by using exposure time dependent spectrum and scattering in the near field methods: how to get fast dynamics with low-speed CCD camera *Opt. Express* **16** 20272–82
- [10] Crococo F and Brogioli D 2011 Quantitative Fourier analysis of Schlieren masks: the transition from shadowgraph to Schlieren *Appl. Opt.* **50** 3419–27
- [11] Goodman J W 2009 *Speckle Phenomena in Optics: Theory and Applications* (Greenwood Village, CO: Roberts and Company)
- [12] Giglio M *et al* 2001 Near-field intensity correlations of scattered light *Appl. Opt.* **40** 4036–40
- [13] Brogioli D *et al* 2009 Nanoparticle characterization by using tilted laser microscopy: back scattering measurement in near field *Opt. Express* **17** 15431–48
- [14] Brogioli D *et al* 2009 Characterization of anisotropic nano-particles by using depolarized dynamic light scattering in the near field *Opt. Express* **17** 1222–33
- [15] Cerbino R and Trappe V 2008 Differential dynamic microscopy: probing wave vector dependent dynamics with a microscope *Phys. Rev. Lett.* **100** 188102-1–4
- [16] van de Hulst H C 1957 *Light Scattering by Small Particles* (New York: Dover)
- [17] Moitzi C *et al* 2009 A new instrument for time-resolved static and dynamic light-scattering experiments in turbid media *J. Colloid. Interface Sci.* **336** 565–74
- [18] Pusey P N 1999 Suppression of multiple scattering by photon cross-correlation techniques *Curr. Opin. Colloid Interface Sci.* **4** 177–85
- [19] Sutton M 2008 A review of X-ray intensity fluctuation spectroscopy *C. R. Phys.* **9** 657–67
- [20] Sutton M *et al* 1991 Observation of speckle by diffraction with coherent x-rays *Nature* **352** 608–10
- [21] Mochrie S G J *et al* 1997 Dynamics of block copolymer micelles revealed by x-ray intensity fluctuation spectroscopy *Phys. Rev. Lett.* **78** 1275
- [22] Cerbino R *et al* 2008 x-ray-scattering information obtained from near-field speckle *Nat. Phys.* **4** 238–43
- [23] Nugent K A 2010 Coherent methods in the X-ray sciences *Adv. Phys.* **59** 1–99